

# **Numerical Simulation of Axisymmetric Jet Screech tones for various Mach Numbers**

*A Graduate Project Report submitted to Manipal Academy of Higher  
Education in partial fulfilment of the requirement for the award of the  
degree of*

**BACHELOR OF TECHNOLOGY**

**In**

**Aeronautical Engineering**

*Submitted by*

**Rithik R Nambiar**

**180933178**

**Karthik Sankar K**

**180933188**

*Under the guidance of*

**Dr. Manoj T Nair**

Professor

Department of Aerospace

Engineering

Indian Institute of Space Science and

Technology

**Dr. Chandrakant R Kini**

Professor

Department of Aeronautical

and Automobile

Engineering

MIT Manipal



**MANIPAL INSTITUTE OF TECHNOLOGY**

**MANIPAL**

*(A constituent unit of MAHE, Manipal)*

**DEPARTMENT OF AERONAUTICAL AND AUTOMOBILE ENGINEERING**

**JULY 2022**

## **ACKNOWLEDGEMENTS**

The satisfaction and euphoria that accompany the successful completion of any task would be incomplete without the mention of the people who made it possible, whose constant guidance and encouragement aided us for the completion.

We would like to thank Dr. Manoj T Nair (Professor, Department of Aerospace, Indian Institute of Space Science and Technology) for providing this invaluable opportunity to work under his guidance. We are grateful to him for his constant support and helping us out during the problems we faced in course of our research project.

Internal guide, Dr. Chandrakant R Kini, and Examiner Mr. Manikandan M, for providing us with valuable support and guidance throughout the project timeline. We would like to this opportunity to thank all the lab assistants of PG Mechanical CAD lab and friends for their valuable support and inputs to this project.

## ABSTRACT

In the history of aviation, supersonic aircraft produced noise which caused severe impacts on the environment. The consequences were majorly on the living organisms and the building structures. Pressure waves from a supersonic plane led to variation in pressure changes on the ground, termed Sonic Boom. According to aviation researchers, based on the intensity of the sonic boom, tall building structures' life span reduces as these pressure waves interact with the surface of buildings. Nowadays, scientists are trying to bring forth new design configurations to reduce the disturbance and increase the efficiency of aircraft. For high performance aircrafts, the noise levels are of a big concern for communities like airbases, staffs, pilots and other related personnel working with this aircraft. For Certification procedures, these are very important factors to look upon.

Noise generated from the supersonic jet is differentiated into three components which are Broadband shock-associated noise, turbulent mixing noise and finally screech tones. Screech tones are discreet high-frequency waves radiated from a supersonic jet than originates from an acoustic feedback loop between the engine and first shock cell. Screech tones are found in under-expanded jets way stronger as in over-expanded they are essentially free of screech. Currently, screech tones can be predicted but there is no mathematical formulation to detect intensity and direction. This research study is focusing on accurately predicting screech tones from a supersonic jet.

Steady-state analysis of supersonic jet is carried out for calibration of the model. For detecting screech tone from the nozzle exit transient formulation is to be deployed. The data is retrieved from the file and is post-processed in CFD-Post. A fast Fourier transform plot is used to plot the data from the microphone location.

Analyzing the FFT plot, screech tone is predicted, and it is compared with the experimental data. The software used is ANSYS WORKBENCH 2022 R1. FLUENT is used for simulating the jet flow and CFD-Post is used for post-processing.

# TABLE OF CONTENTS

	Page	
	No	
Acknowledgment	ii	
Abstract	iii	
List Of Tables	vi	
List Of Figures	vii	
<b>Chapter 1</b>	<b>INTRODUCTION</b>	
1.1	Introduction	1
1.2	Relevance of the work	3
1.3	Objectives	3
<b>Chapter 2</b>	<b>BACKGROUND THEORY LITERATURE REVIEW</b>	
2.1	Background Theory	4
2.2	Literature Review	7
2.3	Research Gap	9
<b>Chapter 3</b>	<b>METHODOLOGY</b>	
3.1	Software used	10
3.2	Problem Description	10
3.3	Flow of work	11
3.4	Meshing	12
3.5	Setting up the model	13
3.6	Cell zone and Boundary Conditions	13
3.7	Solution Methods, Controls, and Initialization	15
3.8	Full Multi-Grid Initialization	16
3.9	Steady state calculation	16
3.10	Transient state calculation	16
3.11	Acoustic Post-processing	16
3.12	Fast Fourier Transform Plot	17

<b>Chapter 4</b>	<b>RESULTS AND DISCUSSION</b>	
4.1	Pressure contour in upstream direction	18
4.2	Steady state analysis	18
4.3	Transient state analysis	21
4.4	Sound pressure level analysis	22
<b>Chapter 5</b>	<b>CONCLUSION AND FUTURE SCOPE OF WORK</b>	
5.1	Conclusion	25
5.2	Future Scope	25
<b>REFERENCES</b>		<b>28</b>

## LIST OF TABLES

<b>Table No</b>	<b>Table Title</b>	<b>Page no</b>
3.1	Microphone location coordinates	<b>12</b>
3.2	Realizable K-epsilon model constants	<b>13</b>
3.3	Datasheet of boundary conditions	<b>14</b>
3.4	Gauge total pressure of corresponding mach number	<b>14</b>
3.5	Relaxation factor datasheet	<b>15</b>
3.6	Data for flow Initialization	<b>15</b>
3.7	Transient flow iteration parameters	<b>16</b>

## LIST OF FIGURES

<b>Figure No</b>	<b>Figure Title</b>	<b>Page No</b>
1.1	Typical far-field narrow-band supersonic jet noise spectrum	2
2.1	Schematic diagram of the screech tone feedback loop	7
3.1	Line Diagram of the geometry	10
3.2	Flow chart of steady-state analysis	11
3.3	Flow chart of transient-state analysis	11
3.4	Meshing domain with dimensions	12
3.5(a)	Mesh Display	13
3.5(b)	Enlarged view of meshing at nozzle exit area	13
4.1	Pressure field contour plot for showing radiation of screech tones. M=1.2	18
4.2	Shock-cell structure of Steady-state at Mach= 1.2	19
4.3	Shock-cell structure of Steady-state at Mach= 1.5	19
4.4	Shock-cell structure of Steady-state at Mach= 1.8	20
4.5	Shock-cell formation transient simulation at M =1.2	21
4.6	Shock-cell formation transient simulation at M =1.5	21
4.7	Shock-cell formation transient simulation at M =1.8	22
4.8	Spectral Analysis of Mic-1 for M = 1.2	22
4.9	Spectral Analysis of Mic-2 for M = 1.2	23
4.10	Spectral Analysis of Mic-1 for M = 1.5	23
4.11	Spectral Analysis of Mic-2 for M= 1.5	23
4.12	Spectral Analysis of Mic-1 for M=1.8	24
4.13	Spectral Analysis of Mic-2 for M=1.8	24

# CHAPTER 1

## INTRODUCTION

### *1.1 Introduction*

The branch of acoustics in which noise generation via aerodynamic forces interact with surfaces or turbulent fluid is called Aeroacoustics. Aeroacoustics focuses on the production and distribution of sound by liquids. The prefix aero means air, but one can also add sound to other liquids, such as water (also called hydroacoustic). Aeroacoustics is part of a broader acoustics theme, the latest of which can include audio streaming with other types of media, including solid, plasma, etc. This research focuses on producing, distributing, and reducing the noise made by engineering and biological systems. With a combination of theory and arithmetic, we analyse complex systems with a physics-based perspective, usually solving Navier-Stokes stressors with two or three sides directly.

Aeroacoustics is an integral part of aerospace vehicle construction, certification, and performance. In commercial aircraft, the noise from the engines affects the way the aircraft is operated inside and near the airport and whether the aircraft is quiet enough to meet the certification requirements. In military aviation, especially passenger planes, aircraft proximity to personnel creates communication challenges and poses a significant health risk of hearing loss. The sound can be generated by jets, fans, rotor blades, etc.

Acoustic noise is any sound in an acoustic background, either intentional or unintentional. Conversely, the noise in electronics may not be audible to the human ear and may require detection tools. Noise is the unwanted sound that is unpleasant, loud, or disturbing. From the physical view of point, there is no distinction between sound and noise required, as both are vibrating in a certain way, such as air or water. The difference arises when the brain receives and hears the sound. The field of jet noise focuses on turbulent eddies caused by shear flow and high-velocity jets in aeroacoustics. It is responsible for the loudest sounds humankind has ever produced.

There are various aspects of acoustics that profoundly affect a person's health. The negative element creates noise. Noise sound waves that are unpleasant to the human ear. Both noise and noise are vibrations that require a medium to move, but differences arise when the brain interprets vibrations. Noise pollution at airports due to flying flights, noise enhanced by adults, tired industrial machinery parts, moving trains, construction sites, etc., can cause a lot of disruption to plants and animals in and around the region. Noise can cause severe damage to human and animal hearing and can cause psychological harm impacts on them. Noise can also cause damage to buildings such as tall buildings, bridges, etc. (For example, a sonic boom from a plane can cause significant damage to buildings.).

The supersonic sound of the jet consists of three main parts: mixed noise with chaos, expansive accompanying shock sound, and screech tones—different Screech tones noise frequency. With low numbers of Supersonic Mach, screech tones are associated with axisymmetric oscillations of the jet and are driven primarily upstream. The partially extended supersonic jet broadcasts both broadband and frequency sound called screech tones. Screech tones are known to produce a response loop driven by a high degree of unstable jet flow waves. Inside the jet plume, there is a quasiperiodic shock cell structure. Instability interactions, waves, and shock cell structure, as the first spreads to the latter, are responsible for generating tones

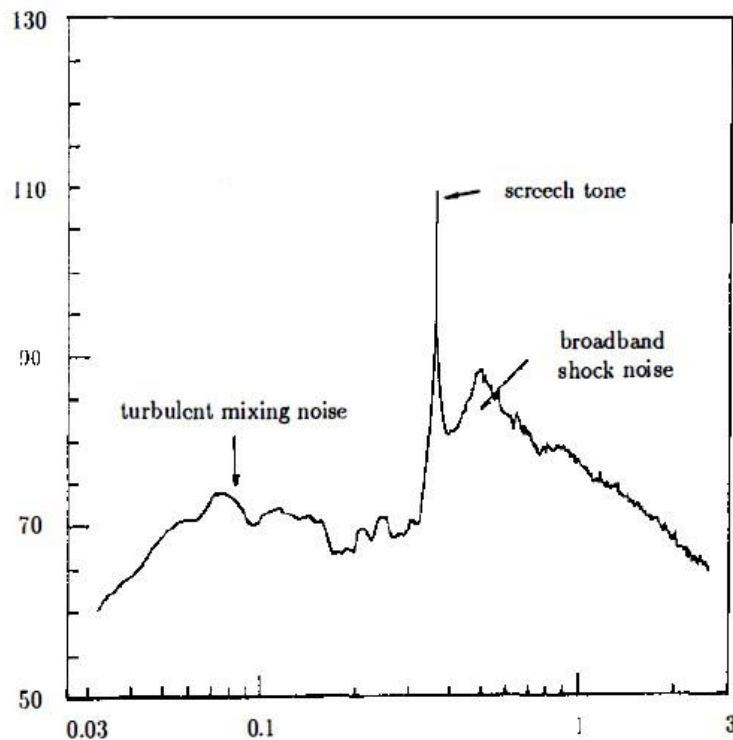


Fig 1.1 Typical far-field narrow-band supersonic jet noise spectrum (Seiner 1984)

Average speed profiles and the shock distribution of the shock cell jet are found to be consistent with the test values. The same is true of the frequency of simulated screech. The intensity of the screech tone and the direction of the jet selected Mach numbers were reported. It is known that screech tones are produced with a response loop. Recent works show that the feedback loop is the same driven by waves of jet flow instability. The source of the partially extended jet is a structure of a quasiperiodic shock cell. Near the tip of the microphone, where the jet mixing layer is thinner and more receptive to external stimuli, the acoustic pressure pressures in this area are pleasing. Waves of instability. Waves of stable and unstable waves from a small flow multiply as they spread out on the ground. After spreading the range of four to five shock cells, a wave of instability after finding the amplitude large enough interacts with quasiperiodic shock cells in the jet plume. Indirect interaction produces acoustic radiation, part of which spreads out of the jet. When you reach the nozzle lip region, the acoustic waves delight the

mixed layer of a jet. This leads to a generation of new waves of instability. This way, the feedback loop is closed.

### *1.2 Relevance of the work*

Currently, there is a reliable screech tone prediction formula. However, there isn't any known way to predict the intensity of the tone and direction, though it is strong. This is not surprising because tone intensity is determined by inconsistency with the response loop. Currently, some formulas can accurately predict tone frequency. However, there is no well-known way to predict the intensity of a screeching tone. In this work, the axisymmetric screech phenomenon of aircraft with a low supersonic Mach number is also produced by imitating numbers.

### *1.3 Objectives*

The objective of this research is to

- Determine the jet shear layer in steady-state and transient-state
- Predict the screech tone modes
- Determine the screech tone frequency for the under-expanded supersonic jet at different Mach numbers from different microphone locations

## **CHAPTER 2**

### **BACKGROUND THEORY AND LITERATURE REVIEW**

#### *2.1 Background Theory*

Computational aeroacoustics (CAA) is a branch of acoustics that aims to analyse noise generation by turbulent flows through numerical methods. Computational Aeroacoustics (CAA) is a study of problems with aeroacoustics using integration techniques. In such computer techniques, like other problems with liquid mechanics, the potential insight gained is more significant if the focus of attention remains a physical problem; counting is viewed as a tool or method for learning aeroacoustics problems. Needless to say, new body test problems bring the need for improvement or improvement calculation techniques to be used. Thus, development takes place, and it is beneficial to maintain a strong link between simulation (number model), a relevant physical problem, and a real-world engineering program that fuelled the problem. This means that the calculation methods are considered as one of many ways to deal with an existing situation, as well alternatives (e.g., theory analysis, model, and full tests) are not excluded but are exploited separately. Power is given by counting methods, numerical issues to be provided careful attention, and one of the latest advances in resolving indirect aeroacoustics problems is being discussed.

A jet sound component called Broadband shock-associated noise (BBSAN) is produced when supersonic jets operate without design. In this research article, a new model called the Reynolds average Navier-stokes (RANS) was introduced to predict broadband noise relief (BBSAN). This model was able to overcome the limitations generated by the empirical model. For a RANS model to develop solutions, it needs geometry and its operating condition. RANS is a numerical method for showing the volatile flow in which flow values are divided into their measured and variable components (Reynolds decay).

The Navier-Stokes statistical index reveals the Reynolds indirect pressure term that requires additional modelling to resolve the Turbulence model fully. Most (if not all) models of RANS disorder are based on robust observations. Navier-Stokes statistics are undoubtedly among the most complex objects in mathematical physics to be applied and solved. This timeline of non-linear calculations requires multiple scales to achieve analytical solutions, and not all systems can be solved. In more common systems or complex geometries, numerical methods are needed to solve these problems and obtain helpful flow behaviour information. Some mathematical calculations can reduce the complexity of these calculations, which will help to speed up simulation without losing much accuracy.

Reynolds-average Navier-Stokes (RANS) stats are a reduced form of standard Navier-Stokes statistics. In the RANS calculations, the fixed position solution is differentiated from the ever-changing fluctuations in the system, which will confuse different flow areas. The further deception of the results of the RANS and the more aggressive models produces many other CFD models, some of which fall into the use of open source and commercial CFDs.

The method used to obtain RANS figures is called the Reynolds decomposition. Reynolds rating and Reynolds decay do not directly refer to Reynolds' number change but rather to the use of the Navier-Stokes mathematical timeline. Time measurement is often used to reduce complex mathematical systems into simpler forms by gradually or eliminating time fluctuations. In this case, the RANS calculations use a solution divided into the flow rate of the independent definition and the time variation in the definition, or

$$u(x, t) = \bar{u}(x) + u'(x, t) - (1)$$

With this decay, one can use some special operators and a time-measuring function to get this non-linear equation that describes flow (in tensor notation):

$$\rho \bar{u}_j \frac{\partial \bar{u}_i}{\partial \bar{u}_j} = \rho \bar{f}_1 + \frac{\partial}{\partial x_j} [-\bar{p} \delta_{ij} + 2\mu \bar{S}_{ij} - \overline{\rho u'_i u'_j}] - (2)$$

Although this model can be very complex, it also offers some freedom to use the model in specific situations where certain words in the strain and stress additions can be ignored. This requires an additional model of confusion to follow these indirect terms in stress tensor. Many of these disturbing models used in RANS ratings are determined by solid perception rather than taken from the original principles. Acoustic waves emanating from an extended jet are characterized by

- Part of the noise is due to the turbulent flow of the flow, which dominates the low waves.
- Part of the broadband noise is due to the presence of shock dominant over high frequencies.
- Smart screech sound.

In 1953, Powell discovered the presence of screaming tones.” The accompanying vortical structures that grow in the shear layers are transported downstream and interact with alarming cells that produce powerful acoustic waves. The interaction between such noisy waves propagating over the mouth with a microphone and a thin shaving layer stimulates new unstable waves that flow downstream and close the response loop”. In this journal, the distance from the exit of a plane to a critical area is considered large enough to produce screech tones. When the installation is close to the nozzle, a change in jet oscillation status is observed.

Analysing the flow field, there are three circuits, an uninterrupted circuit, a region near the plate where the speed decreases and the shock absorber is adjusted, and a circuit with a radial flow in the curve. This article gives us insight into the aeroacoustics response method of supersonic impinging jets planar using a large eddy simulation (LES). Different impact angles are considered, and their reaction mechanism between the nozzle tip and the flat plate is observed. Several tones can be seen in the compression area. If there is a change in the impact angle, a decrease in strength is observed. This article helps to build on further development in the future. The axisymmetric analysis is a less expensive form of jet screech sound, but this method can only be accepted in low-frequency Supersonic Mach cases where the screech tone modes are axisymmetric. At higher Mach numbers, screech tone modes distributed by the axisymmetric microphone become a 3D object with helical vibrations or blows.

The K-epsilon (k-ε) turbulence model is primarily used in computational fluid dynamics (CFD) to mimic the flow characteristics of the definition of flow conditions. A two-dimensional model provides a standard definition of chaos using two transport statistics (partial numbers, PDEs). The initial impulsion for the K-epsilon model was to develop a mixing-length model and find another way to define the mean lengths of the equilibrium to moderate to high flow. The first variable turbulent kinetic energy (k). The second variable transport rate is the dissipation kinetic energy dissipation (ε).

Turbulent Kinetic Energy (k):

$$\frac{\partial(\rho k)}{\partial t} + \frac{\partial(\rho k u_i)}{\partial x_i} = \frac{\partial}{\partial x_j} \left[ \frac{\mu_t}{\sigma_k} \frac{\partial k}{\partial x_j} \right] + 2\mu_t E_{ij} E_{ij} - \rho \varepsilon - (4)$$

Dissipation (ε):

$$\frac{\partial(\rho \varepsilon)}{\partial t} + \frac{\partial(\rho \varepsilon u_i)}{\partial x_i} = \frac{\partial}{\partial x_j} \left[ \frac{\mu_t}{\sigma_\varepsilon} \frac{\partial \varepsilon}{\partial x_j} \right] + C_{1\varepsilon} \frac{\varepsilon}{k} 2\mu_t E_{ij} E_{ij} - C_{2\varepsilon} \rho \frac{\varepsilon^2}{k} - (5)$$

K-ε Realizable is used in the analysis because it provides an advanced prediction of your spread rate for both flat and circular jets. It also exhibits high flow efficiency, including rotation, boundary layers under strong gradients, splits, and rotation. In almost all comparative measurements, Realizable k-ε demonstrates the high ability to capture the total flow of complex structures. Also, Sutherland's law of viscosity which is a dependence of viscosity of gases on temperature, is used. For high temperatures, the temperature dependence of viscosity (Sutherland's law) can significantly impact the flow.

We are using Green-Gauss Node-based method because this method is more accurate on meshes with higher mesh skewness. In most cases you should be using the Least-Squares Cell-based methods, however, which should be faster (and more accurate) than the Green-Gauss Node Based Gradient method, at least on static meshes, in the most cases. It is also highly beneficial if you have dynamic mesh. We also use Ffowcs-Williams & Hawkings just to make Sound pressure levels available for FFT spectral analysis. It is Lighthill's jet noise equation's generalization.

## 2.2 Literature Review

Christopher K.W. Tam [19] explains in his research on supersonic jets that it is now generally accepted that turbulent jet flows contain both fine and large scales of turbulence. Both structures are productive noise. The relative importance of the sound they make, however, depends largely on jet Mach number and the temperature. Most of these jets are under-expanded. He further added that the Presence of sound reflecting surfaces like impingements in the jet environment, Mach number of the jet, the thickness of nozzle lip, and temperature of the jet affects the screech tone intensities. Further explanation of the screech tone generation mechanism was explained. The acoustic feedback phenomenon was the reason for the screech tones to be observed. The acoustic disturbances advance near the nozzle lip where there's a thin jet mixing layer and external excitation can be received. At the nozzle exit, the amplitude of excited instability is small. As it propagates downstream, the instability wave extracts energy and rapidly grows. After propagating four to five shock shells, large enough amplitude would be acquired and with the quasiperiodic shock cells in the jet plume. Acoustic radiation generates due to this unsteady interaction. This radiation is primarily in the upstream direction in the case of Broadband shock associated noise and the acoustic wave feedback travels upstream outside the jet generating new instable waves. Thus, feedback loop is closed.

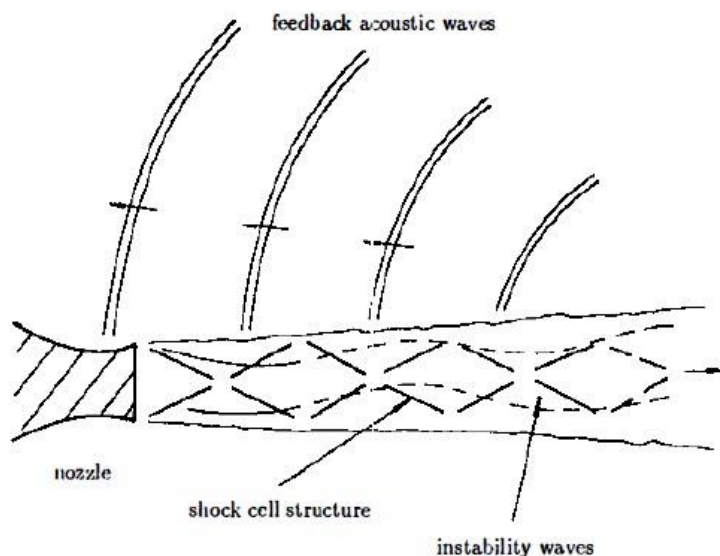


Fig 2.1 Schematic diagram of the screech tone feedback loop. (Christopher K.W Tam)

Hao Shen and Christopher K. W. Tam demonstrated that numerical simulation using computational aeroacoustics methods provides an opportunity to learn the physics and in-depth mechanisms of screech tone intensity and directivity by an entirely new approach by determining the phenomenon in a reliable way [8]. They also mentioned about previous studies stating that numerical simulation of jet noise generation is prone to long scale discrepancies and solving sound flow many-order-of-magnitude variations. Their work showed that by careful design of the computational grid and using high order finite difference scheme, these problems can be controlled.

The K- $\epsilon$  turbulence model is proven for predicting mean velocity profiles of turbulent flows as a very handy engineering approach. There are a lot of papers written on this model. For mean flow calculations and turbulent jet intensity and time scales therefore, to obtain a valuable flow information for predicting noise, this is an excellent method. For this, Bailly and Khavaran adopted this approach. With the usage of empirical constants, K- $\epsilon$  model mixed with Sarkar and Pope corrections for the Mach number range of 0.4-2.0 and jet total temperature ratio ranging 1.0-4.0 provides jet mean flow predictions very accurately. This is applicable for non-axisymmetric and axisymmetric jets. The solution's independence to initial condition is its High Reynolds number jet flows variability and not a setback.

The experimental works are done by Steven A. E. Miller and Philips. J. Morris shares that the often-dominating noise source towards upwards and side-line direction relative to the axis of jet are Broad-Band Shock associated noise and are characterized by more than one broadband peak in the far-field [3]. This happens in the jet shear layers meeting with the shock cell structure by large-scale coherent turbulent structures. Predictions of noise components to RANS equations using a two-equation turbulence model by a BBSAN noise model recently developed by the authors. This model is applied to rectangular and dual streams operating at high temperature, off-design and supersonic. Philips and Steven attempted to overcome the restrictions of older models by reducing empiricism and totally keeping it on RANS CFD predictions.

### *2.3 Research Gap*

The present work is our best understanding of all the research works done earlier on this problem statement and applying the best applications. We are using Computational Aeroacoustics (CAA) to model screech tone noise in an axisymmetric supersonic jet. A K-epsilon ( $k-\epsilon$ ) turbulence model is used to calculate the acoustics of near-field and unsteady flow using Direct CAA. Comparing the screech tone frequencies at  $M=1.2$ ,  $M=1.5$ ,  $M=1.8$  and analyzing how an increase in Mach number affects the sound pressure levels in supersonic jets. The frequency and amplitude of specific nodes are depending on nozzle lip thickness as shown in the works of Ponton and Seiner for Nearfield acoustic measurements. Variable pressure gauges made in the exit of nozzle have acoustic amplitudes above the nearfield microphone dimensions [2]. One of the goals of this study is to understand how nozzle lip thickness causes change in momentum thickness and a better understanding of screech tone behaviors. Further research work can be done on how impingement can be placed downstream from the exit and affection the acoustic behaviors of the supersonic jets.

## CHAPTER 3 METHODOLOGY

This chapter provides an insight into the flow of work and determination of screech tone by a low supersonic free flow jet by Computational Aeroacoustics (CAA). This research aims to detect the screech tone produced by a supersonic free-flow jet for Mach Numbers 1.2, 1.5 and 1.8 and compare the results. The analysis is done on an axisymmetric free jet for a steady-state low supersonic flow. This process calibrates the analysis data for performing transient flow using the Realizable unsteady k- $\epsilon$  model. Spectral analysis is done on the output FFT plot data to determine screech tone.

### 3.1 Software used

ANSYS is an industrial-level engineering tool comprising digital-level functions widely used in research and development across reputed organisations. It requires complex computation power to simulate sophisticated models accurately.

The version of ANSYS used for the simulation is 2022 R1. Simulation is deployed in ANSYS Fluent and post-processing of data is carried out in CFD-Post.

### 3.2 Problem Description

A Comparative study is being carried out on an axisymmetric jet working at Mach numbers 1.2, 1.5, and 1.8. Round nozzle geometry is considered with a diameter of 1-inch and wall-lip thickness of 0.625-inch. The Microphones are located at 0.642-inch and 0.889-inch along the wall lip to detect the presence of screech tones. Inside geometry of the nozzle is not modelled and the nozzle exit is considered as the inlet for the simulation.

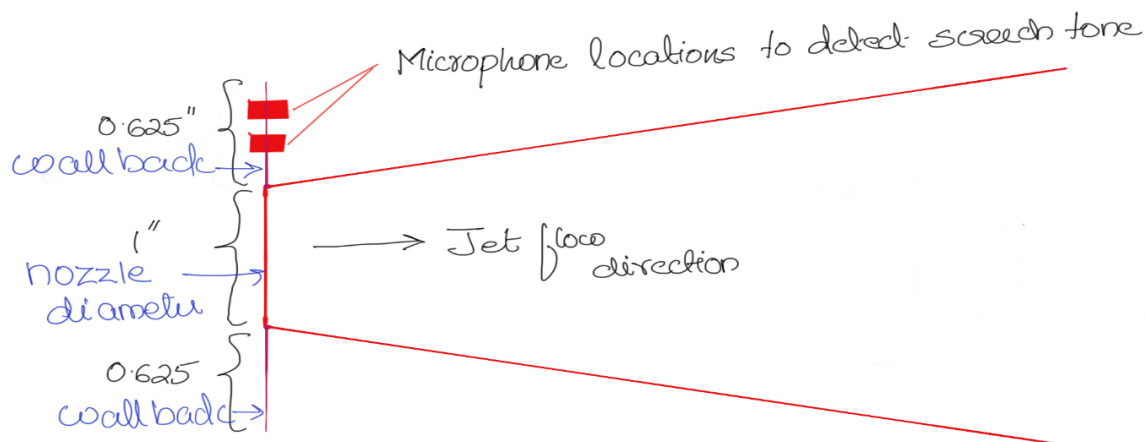


Fig.3.1. Line Diagram of the geometry.

### 3.3 Flow of work

Flow charts help to visualize the procedure very quickly. Figure 3.2 is a flowchart that illustrates the approach taken to analyse the steady-state flow. The steady-state flow is used to calibrate the settings to run the transient flow. In transient, some of the settings are changed. Figure 3.3 illustrates the workflow of transient analysis. The same steps are followed for different Mach numbers.

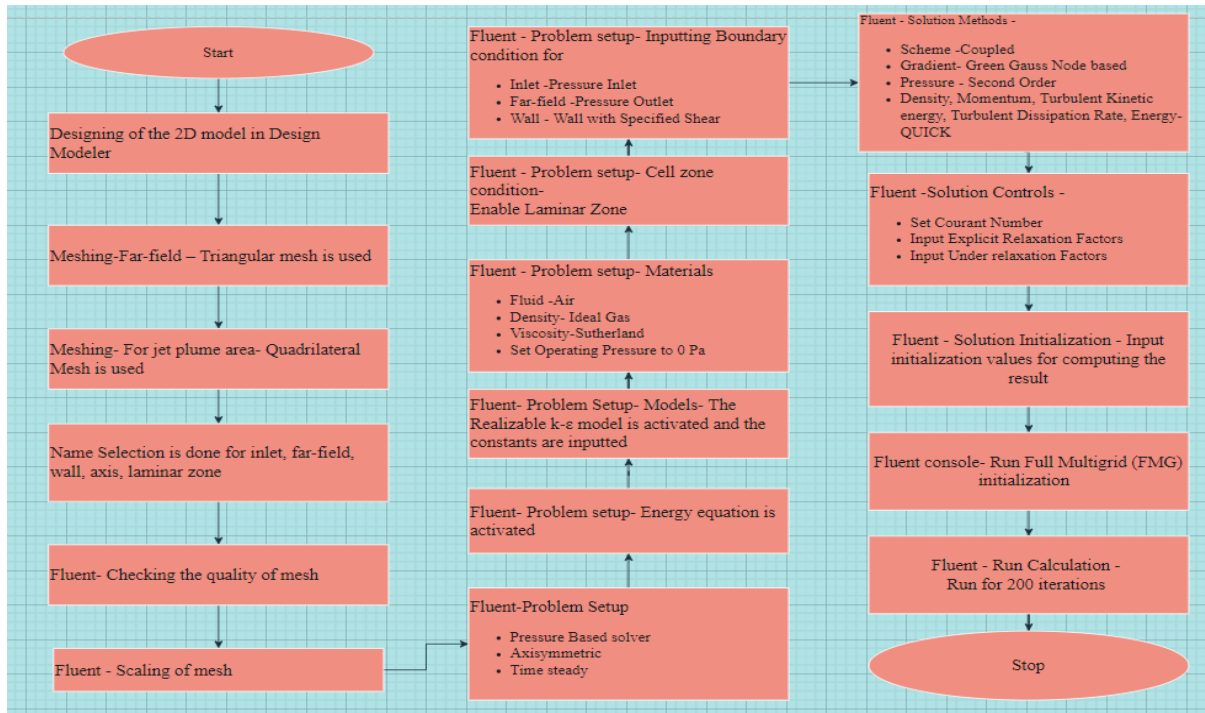


Fig.3.2. Flow chart of steady-state analysis.

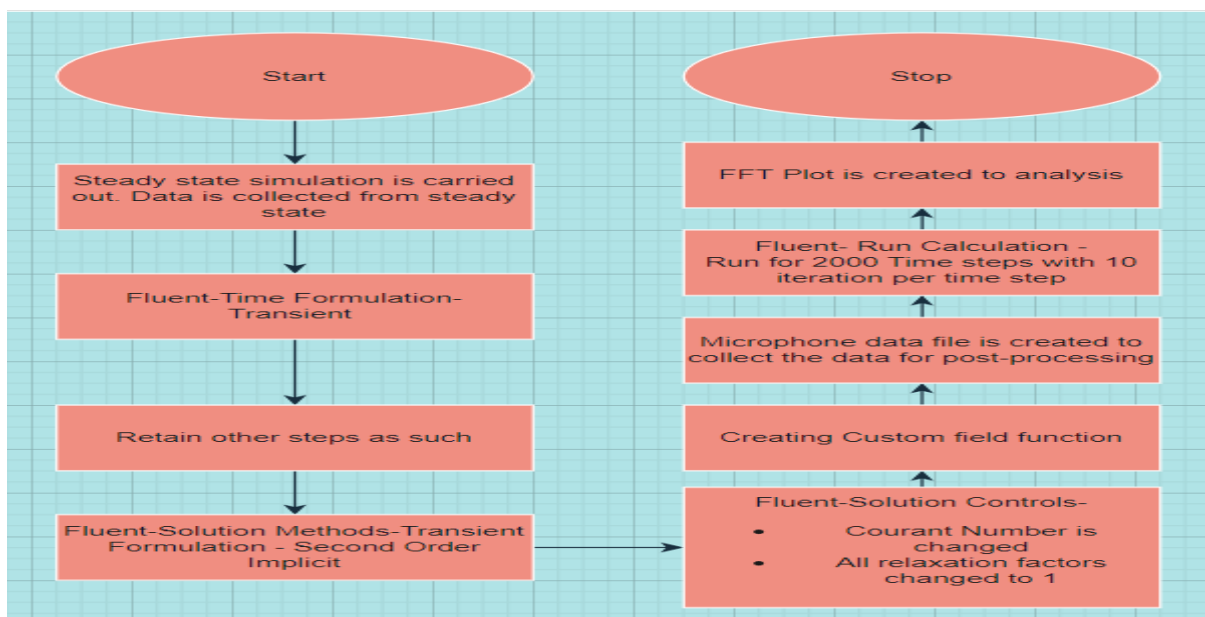


Fig.3.3 Flow chart of transient-state analysis

### 3.4 Meshing

The geometry dimensions of the problem statement are as follows:

- Round Jet inlet diameter – 1 inch
- Wall-lip thickness – 0.625 inch
- Far-field radius – 1000 inch
- Nodes – 1466904
- Elements – 1496645
- Growth rate – 1.2
- Quadrilateral Mesh size –  $1e-04m$
- Triangular Mesh size – 1.5m

Two microphones are placed above the nozzle and along the wall lip. The coordinates of the microphones are given in Table 3.1:

Table 3.1. Microphone location coordinates.

Microphone	X(m)	Y(m)
Mic-1	0	0.0163068
Mic-2	0	0.0225806

Triangular mesh is used for the far-field region with a mesh sizing of 1.5m. The turbulence region or jet plume, and laminar zone use Quadrilateral mesh sizing of 0.0001m. Figure 3.4 depicts the meshing with details of the mesh size. Figure 3.5(a) demonstrates the mesh used and Figure 3.5(b) Enlarged view of the turbulent zone. Small mesh size enables the model to resolve excitations of the jet shear layer at the nozzle tip, generation of shear layer instability waves, formation of shock cell structures in the nozzle core and nearfield propagation of screech acoustic waves.

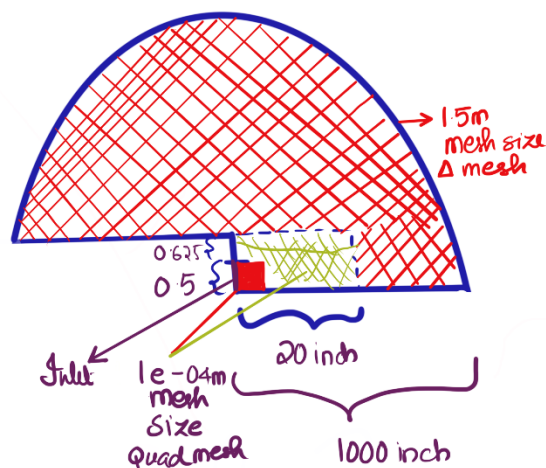


Fig.3.4 Meshing domain with dimensions.

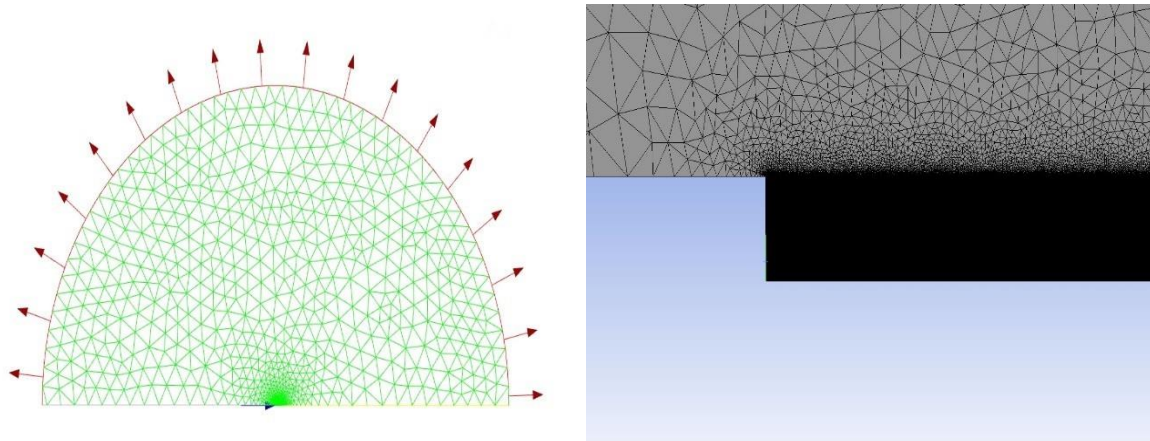


Fig 3.5(a) Mesh Display (b) Enlarged view of meshing at nozzle exit area.

### 3.5 Setting up of model

The mesh generated is checked for quality and is scaled to meters in order to get the analysis results in SI units. The problem statement uses a two-dimensional steady-state axisymmetric model. Pressure-based solver type is used. For structured meshes, the higher-order QUICK discretisation method in CFD offers high resolution for certain parameters like density, energy, and momentum when a Pressure-based solver is used.

The realisable  $k-\epsilon$  viscous model is used with the model constants modified by Tam and Thies for the prediction of turbulent jet flows [1]. This model is highly efficient, and it can deliver results for complex problems. Standard Wall Function is applied for Near Wall Treatment. The modified model constants are shown in Table 3.2:

Table.3.2. Realisable K-epsilon model constants

SI No	Model Constant	Data
1.	C2-Epsilon	2.02
2.	Turbulent Kinetic Energy Prandtl Number	0.324
3.	Turbulent Dissipation Rate Prandtl Number	0.377
4.	Energy Prandtl Number	0.422

### 3.6 Cell Zone and Boundary Conditions

The working fluid considered for this setup is ideally compressed air. The viscosity of air is based on Sutherland's Three Co-efficient method. The density of ideal gas is considered in this case. At the exit of the nozzle, a finitely small region is considered laminar, and the rest of the area is modelled as the turbulent region. The finitely small laminar area is to increase the mixing layer instability waves. Operating pressure is set to 0 Pa.

The next step is to assign boundary conditions. The isentropic relations correspond to the fully expanded jet flying at the specified Mach numbers. Turbulent intensity is taken as 0.1% because turbulence is assumed to be very low at the exit of the nozzle. Since cold jets are considered, the Total Temperature can be assumed to be equal to ambient static pressure. Walls are modelled as slip walls because screech tones are generated by free jet flows and walls do not have much effect. Datasheet of boundary conditions mentioned in the Table.3.3

Table.3.3. Datasheet of boundary conditions.

SI No:	Boundary Name	Type	Parameters
1.	Inlet	Pressure Inlet	<ul style="list-style-type: none"> <li>• Initial Gauge pressure – 127360 Pa</li> <li>• Turbulent Intensity – 0.1%</li> <li>• Hydraulic Diameter – 0.0254 m</li> <li>• Total temperature – 300 K</li> </ul>
2.	Far-field	Pressure Outlet	<ul style="list-style-type: none"> <li>• Gauge Pressure – 100000 Pa</li> <li>• Backflow Turbulent Intensity – 1%</li> <li>• Backflow Turbulent Viscosity Ratio – 2</li> <li>• Backflow Total Temperature – 300K</li> </ul>
3.	Wall	Wall	<ul style="list-style-type: none"> <li>• Shear Condition – Specified Shear <ul style="list-style-type: none"> <li>○ X-component Shear – 0 Pa</li> <li>○ Y-component Shear – 0 Pa</li> </ul> </li> <li>• Roughness Constant – 0.5</li> <li>• Heat Flux – 0 W/m<sup>2</sup></li> </ul>

For calculating Total Gauge pressure at different Mach numbers, we considered static pressure as 100000 Pa and the isentropic relation for pressure is used for determining stagnation pressure which is given as

$$\frac{P}{P_t} = \left(1 + \frac{\gamma - 1}{2} M^2\right)^{\frac{-\gamma}{\gamma - 1}}$$

From the above equation, total stagnation pressure is calculated. The calculated total stagnation pressure for given Mach numbers is given in Table 3.4.

Table 3.4. Gauge Total pressure of corresponding Mach Number

Mach Number	$\frac{P}{P_t}$	Gauge Total Pressure (Pa)
1.2	0.4124	242496.5
1.5	0.2724	367107.2
1.8	0.1740	574712.6

### 3.7 Solution methods, Controls, and Initialisation

In solution methods, for the Pressure-Velocity coupling scheme, the coupled algorithm is used because it obtains a robust and efficient single-phase implementation for steady flows and performance [18]. For transient flows with large time steps, the coupled algorithm is a necessity.

Green-Gauss node-based scheme offers better performance compared to other gradient evaluations. As discussed earlier in this chapter, since a pressure-based solver is used QUICK discretisation of density, momentum and energy enhances the performance.

Courant Number is named after the mathematician Richard Courant. It is a non-dimensional number used in transient simulation to calculate the time step required for the particular size of mesh and flow velocity. For this test case, the courant number is set to 50. Flow initialisation data and relaxation factors data are furnished in the Table 3.6 and 3.5 respectively.

Table.3.5. Relaxation Factors Datasheet

Sl No	Factors	Values
1.	Explicit Relaxation Factors	<ul style="list-style-type: none"> <li>Momentum – 0.25</li> <li>Pressure – 0.25</li> </ul>
2.	Under Relaxation Factors	<ul style="list-style-type: none"> <li>Density – 0.25</li> <li>Body forces – 1</li> <li>Turbulent Kinetic Energy – 0.8</li> <li>Turbulent Dissipation Rate – 0.8</li> <li>Turbulent Viscosity – 1</li> <li>Energy - 1</li> </ul>

Table.3.6 Data for Flow-initialisation

Sl No	Initialisation Parameter	Data
1.	Gauge Pressure	100000 Pa
2.	Axial Pressure	0 m/s
3.	Radial Velocity	0 m/s
4.	Turbulent Kinetic Energy	0.1 m <sup>2</sup> /s <sup>2</sup>
5.	Turbulent Dissipation Rate	6 m <sup>2</sup> /s <sup>3</sup>
6.	Temperature	300 K

### 3.8 Full Multi-Grid initialisation

FMG initialisation can only be used for steady state. In order to accelerate the flow convergence, FMG initialisation provides an initial solution at the beginning of the calculation [18]. At minimal cost, FMG provides an initial and approximate solution when compared to complex computation which increases the computational cost. FMG initialisation code is enclosed in the annexure.

### 3.9 Steady-state Calculation

The steady-state calculation is done for 200 iterations. The result obtained is post-processed in CFD-Post. Mach number contour is plotted, and a steady-state shock structure is obtained.

### 3.10 Transient state calculation

Reading the data results obtained from the steady-state analysis is required to optimize the analysis. For transient analysis, the Time Formulation is changed to Transient. Second-order Implicit is introduced for Transient Formulation in Solution Methods.

It is recommended to increase the value of the Courant number to  $1e-15$  for transient pressure-based coupled solver as the high courant number removes the Implicit Relaxation factors from coupled equations. Explicit and Under-Relaxation factors are set to 1. The parameters for iterating the transient flow are mentioned in the Table.3.7

Table.3.7. Transient Flow Iteration Parameters.

Sl No:	Parameters	Data
1.	Time Stepping Method	Fixed
2.	Time Step Size	5e-06
3.	Number of Time Steps	2000
4.	Maximum Iterations per Time Step	10
5.	Profile Update Interval	1

After 20000 iterations, the post-processing of the simulation is carried out in CFD-Post. Microphone data are collected from the ".out" file and are plotted for spectral analysis using FFT.

### 3.11 Acoustic Post-Processing

A Custom-field function named as "pa" is created to analyse the static pressure perturbations. It is defined as "p-100000". This custom-field function is post-processed in CFD-Post for further reference.

Ffowcs-Williams and Hawkings Acoustic model is deployed. Microphones are defined at different locations in the wall-lip of the jet. This model should be enabled for FFT spectral analysis.

### *3.12 FFT Plot*

Fast Fourier Transform (FFT) plot is used for spectral analysis of generated screech tone. Sound pressure level (SPL) is plotted on the y-axis and frequency is plotted on the x-axis.

## CHAPTER 4

### RESULT ANALYSIS

From numerous complex simulations computed in ANSYS FLUENT, effective and realistic results has been obtained. The input data like k- $\epsilon$  model constants is taken from rigorous research work done by Tam and Thies for effective prediction of supersonic jet flow[1]. The problem geometry, flow constraints and other parameters are taken from research work done by Ponton and Seiner[2]. Lighthill's analogy laid foundation for the computational aero-acoustics which in turn led to prediction of jet screech tone. Research is being extensively done in the field of aero-acoustics to predict the screech tone intensity and direction. Currently, presence of screech tone can only be predicted. This study focuses on efficient prediction of screech tone modes using different model configurations.

#### 4.1 Pressure contour in the upstream direction

The Static-Pressure Perturbation graph which is plotted from the custom field function Pa. This Custom field function contour depicts the propagation of sound waves from the source as observed from the Figure 4.1.

We can understand from the contours that screech tone sound waves travel in the upstream direction. We cannot observe the jet mean flow and radiated sound waves simultaneously because of large inconsistency in amplitude between them in a same contour plot for the same contour limits.

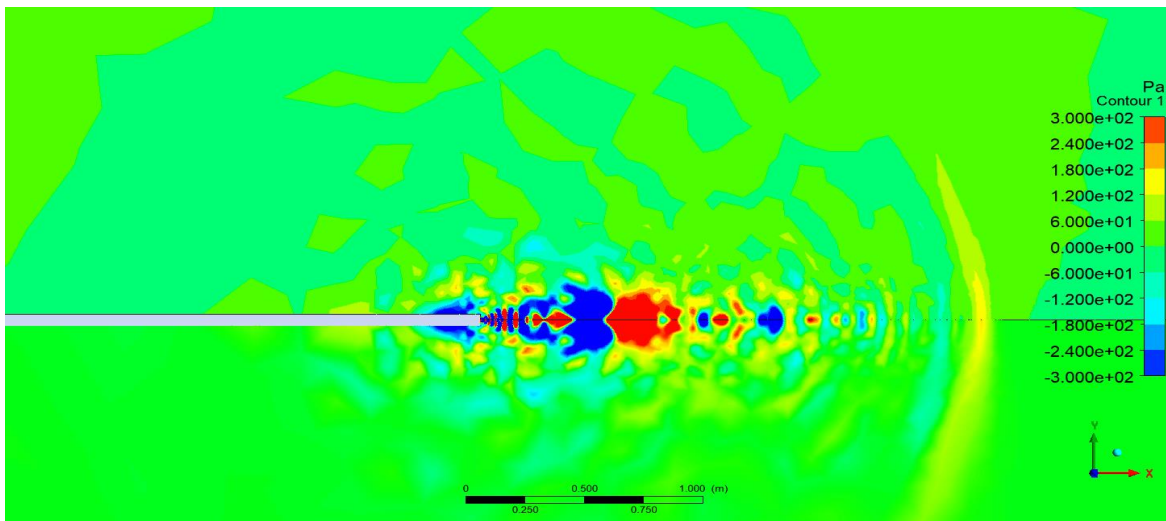


Fig 4.1 Pressure field contour plot for showing radiation of screech tones.  $M=1.2$

#### 4.2 Steady-state analysis

Steady-state analysis for the predicting jet-shear layer is implemented to calibrate the model to simulate transient-state analysis. Figure 4.1, 4.2, 4.3 depicts the velocity contour computed

while simulating steady-state for  $M=1.2, 1.5$  and  $1.8$  respectively. The formation of shock-cell structures from the nozzle exit is seen in the three cases.

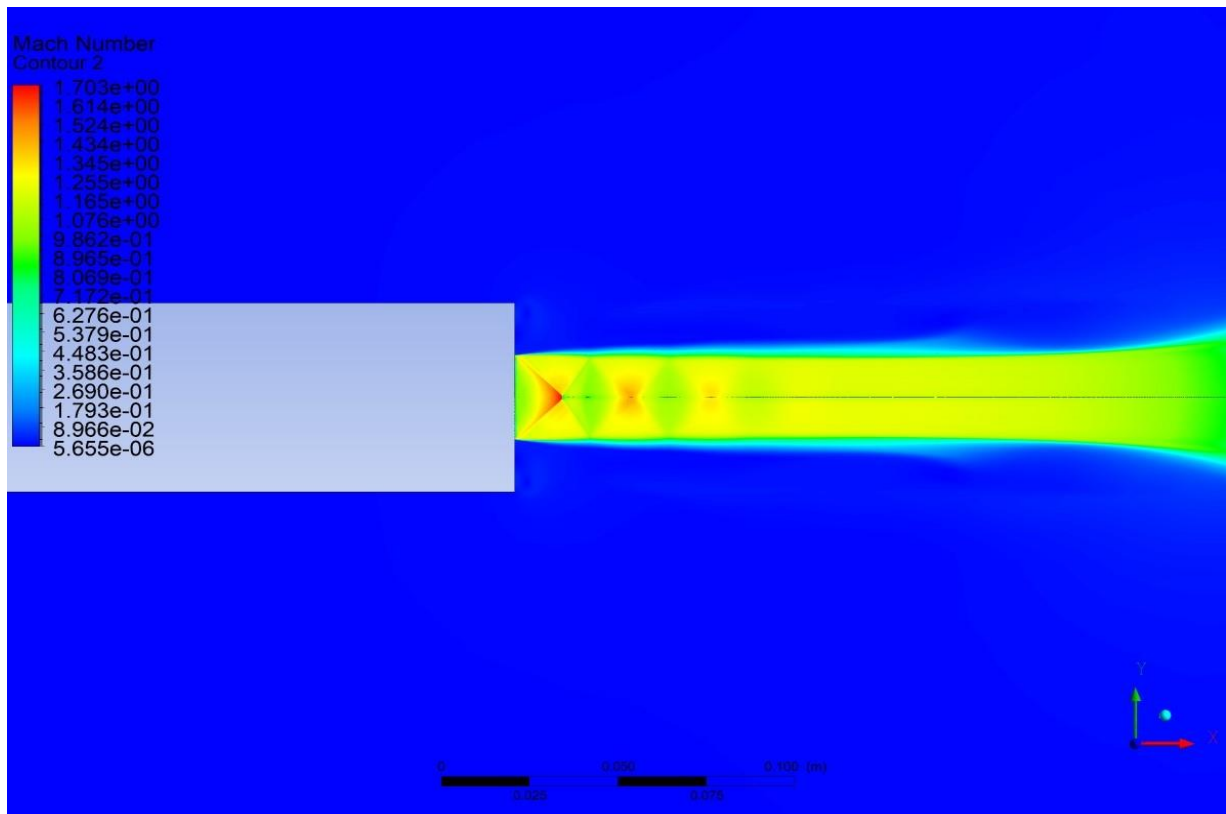


Fig.4.2 Shock-cell structure of Steady-state at Mach= 1.2

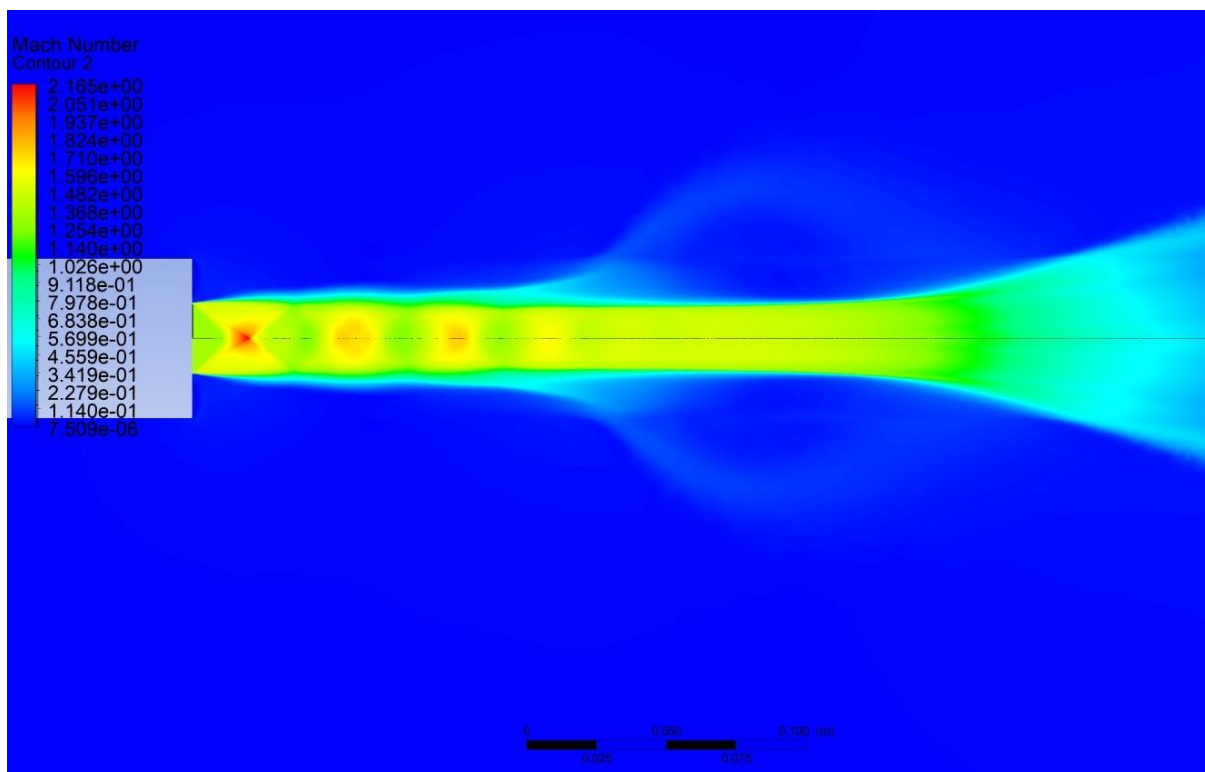


Fig.4.3 Shock-cell structure of Steady-state at Mach= 1.5

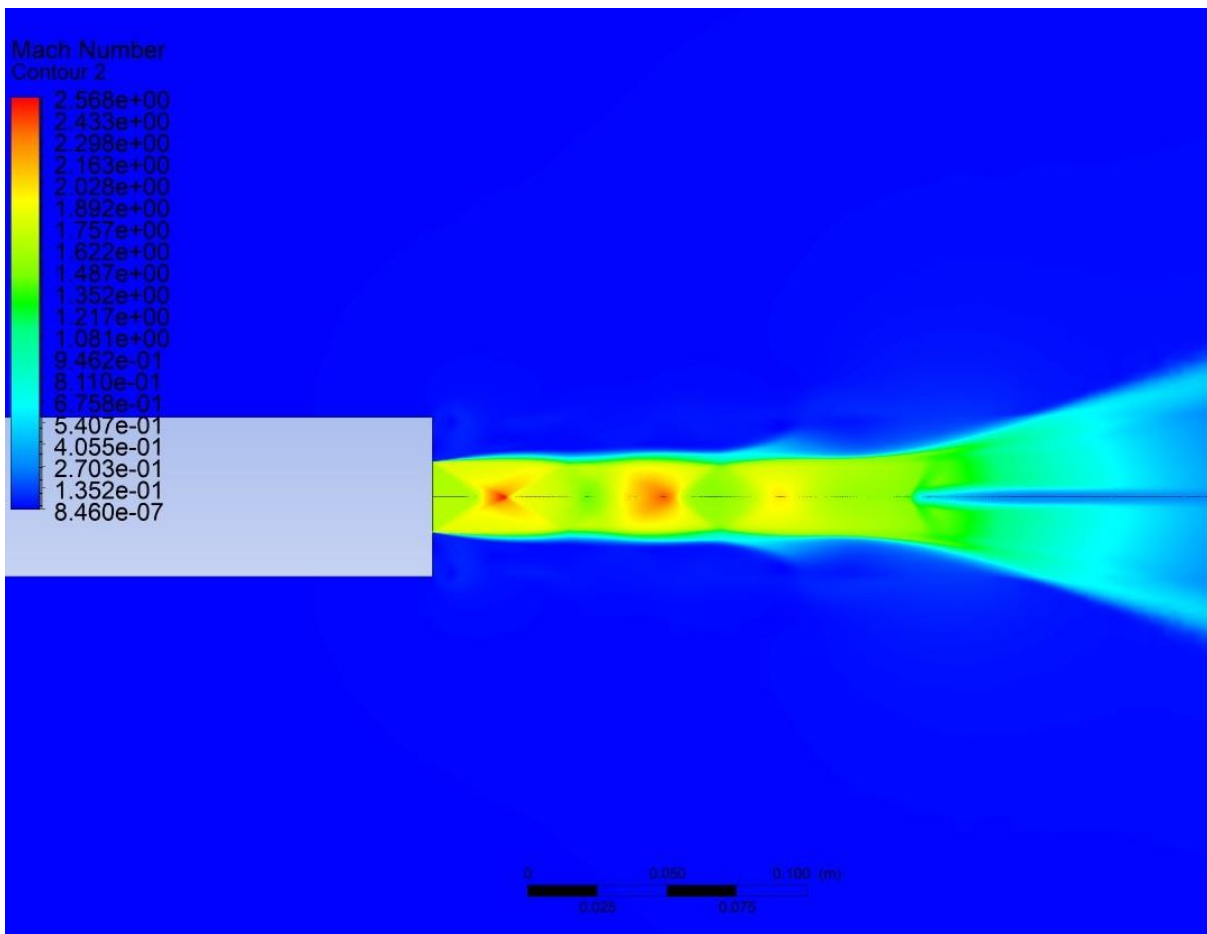


Fig 4.4 Shock-cell structure of Steady-state at M=1.8

From the above figures we can see formation of three to four shock cells for M=1.2, two to three shock cell formations for M=1.5 and roughly two for Mach 1.8 before dissipation. Due to the sensitivity of jet screech mechanism specific to experiment setup, mach number performance can change with each simulation [18]

#### 4.2 Transient-state analysis

It can be observed a difference in the velocity contour of steady-state and transient-state. The shock-cell structure in steady-state is suppressed. Transient simulation provides efficient and more approximate solution than steady-state simulation. Observing the Figure 4.2, transient state shock structure formation can be seen.

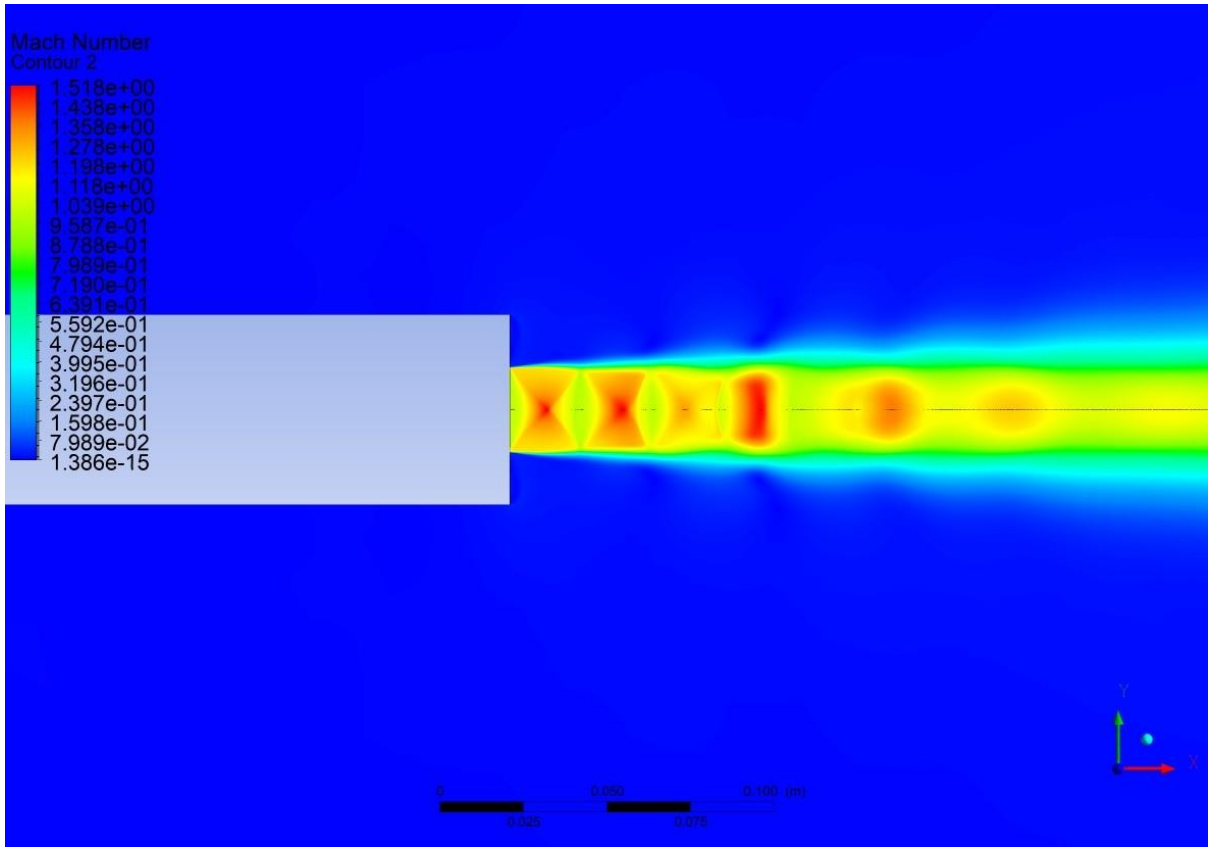


Fig.4.5 Shock-cell formation transient simulation at M =1.2

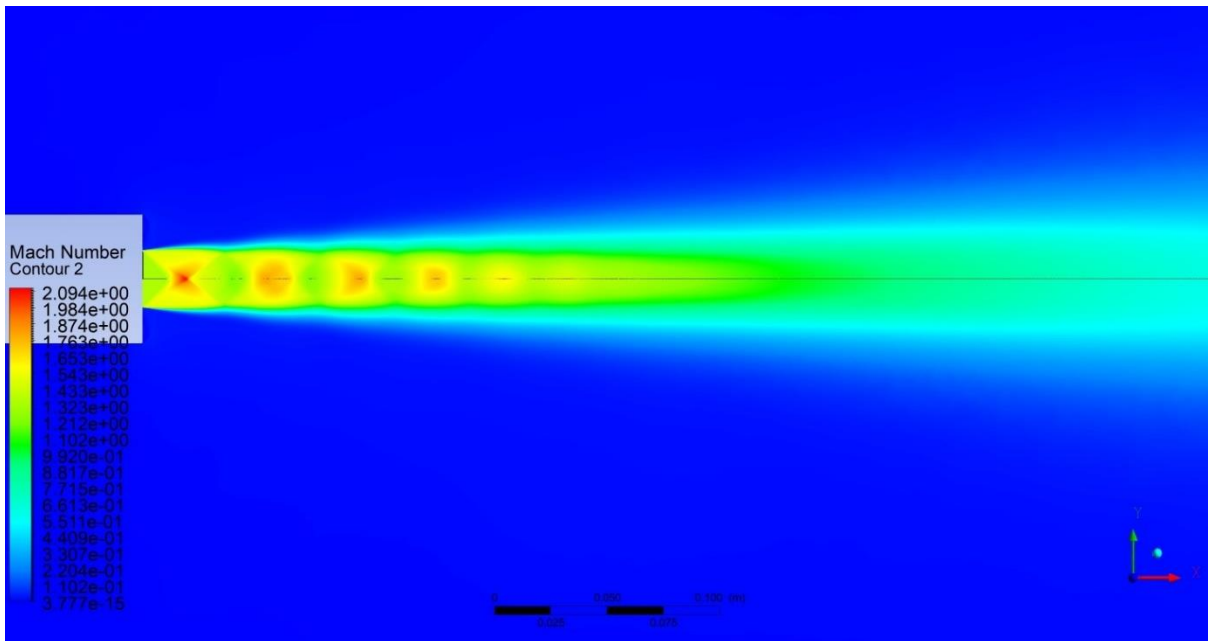


Fig.4.6 Shock-cell formation transient simulation at M =1.5

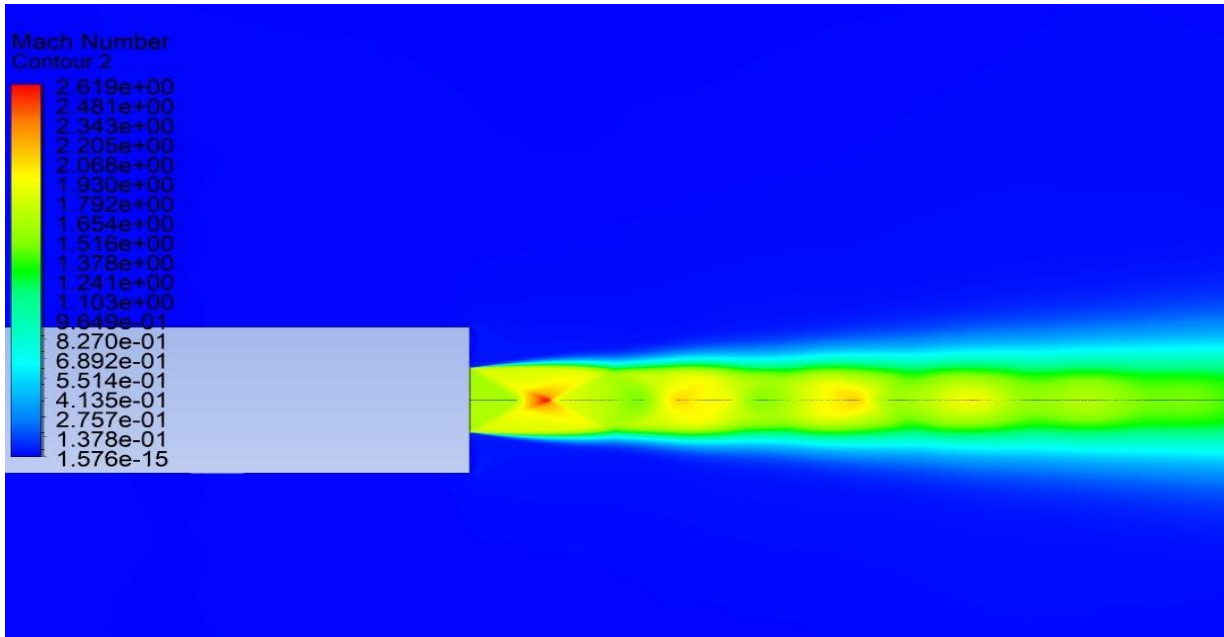


Fig.4.7 Shock-cell formation transient simulation at Mach 1.8

From Fig 4.5, we can see prominent shock cells formation for  $M = 1.2$  whereas the strength of the shock cells decreases moving from  $M= 1.5$  to  $M=1.8$  from Fig 4.6 and 4.7 respectively. We can also observe that shock cell width is smaller for  $M=1.2$  compared to higher mach numbers.

### 4.3 Sound pressure level Analysis

Screech tones found for various mach numbers are shown in SPL vs Frequency graph below:

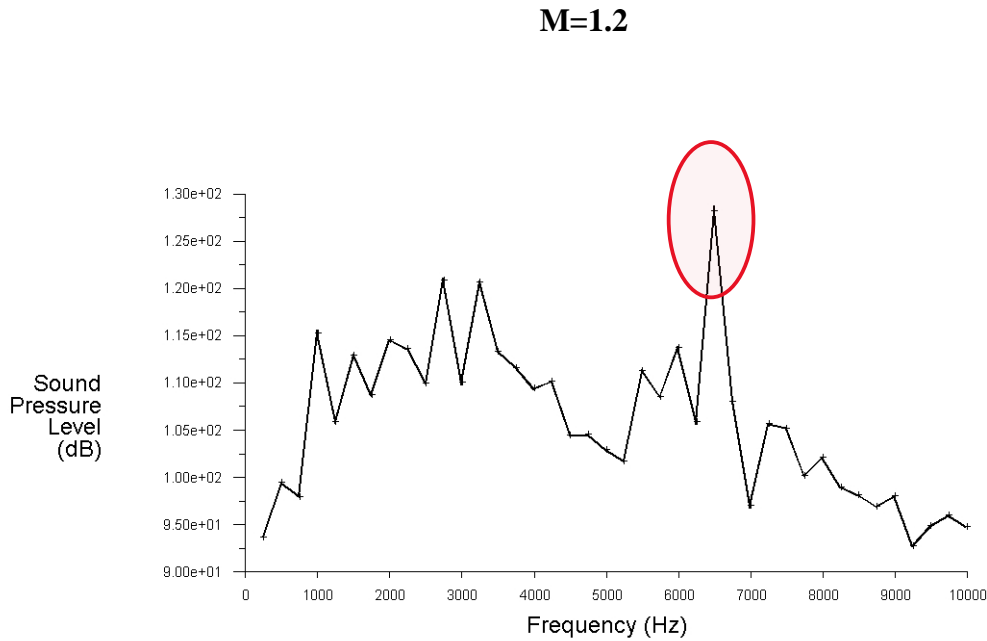


Fig.4.8 Spectral Analysis of Mic-1

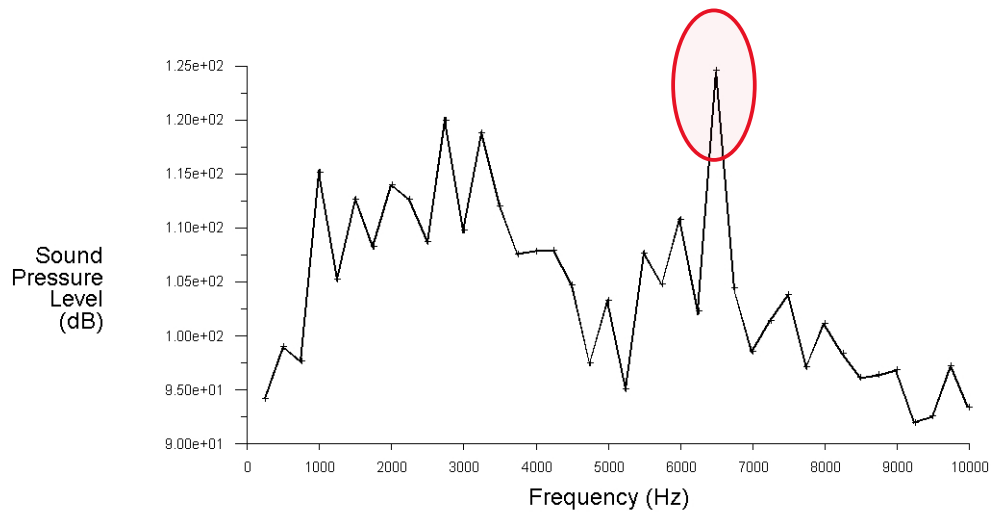


Fig.4.9 Spectral Analysis of Mic-2

**M=1.5**

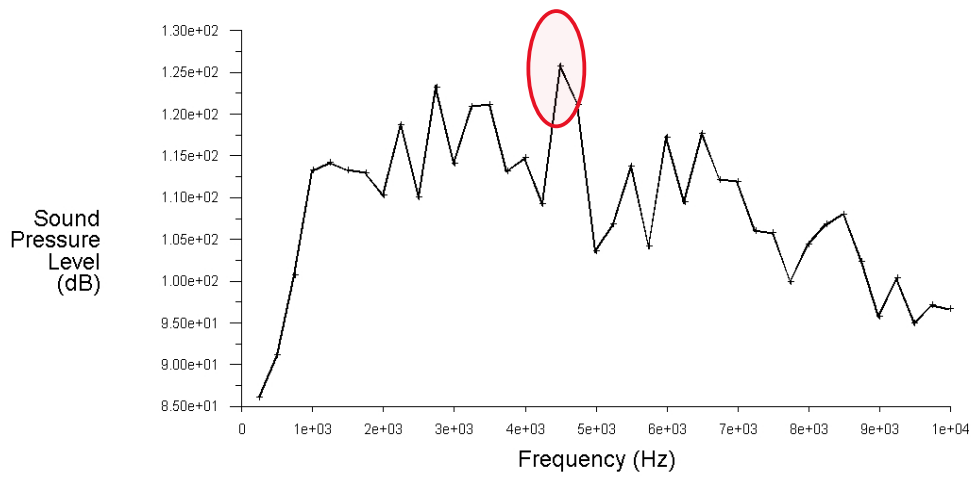


Fig.4.10 Spectral Analysis of Mic-1

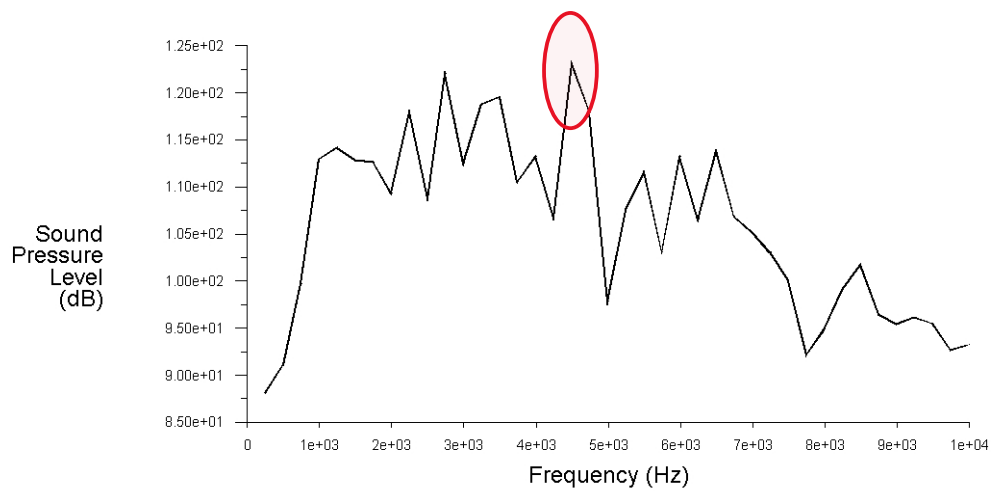


Fig.4.11 Spectral Analysis of Mic-2

**M=1.8**

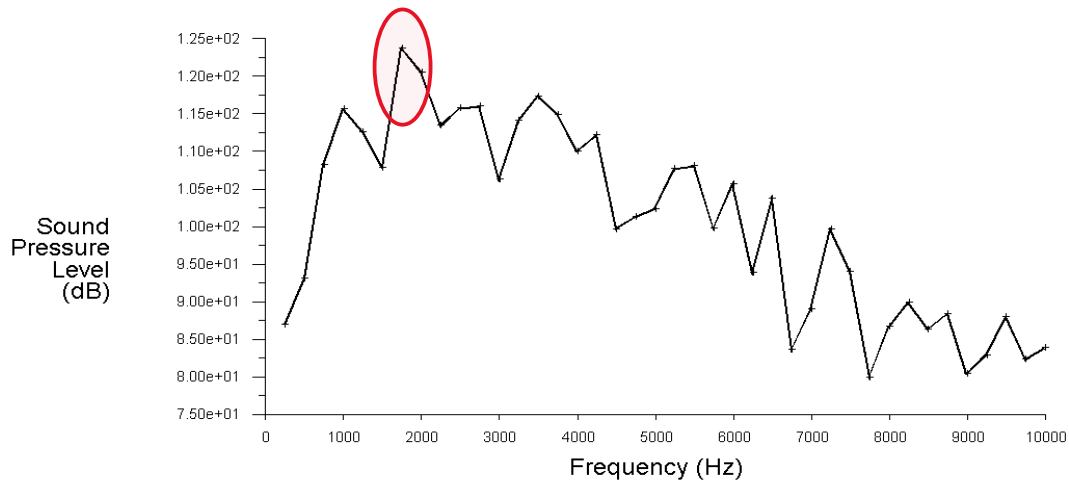


Fig.4.12 Spectral Analysis of Mic-1

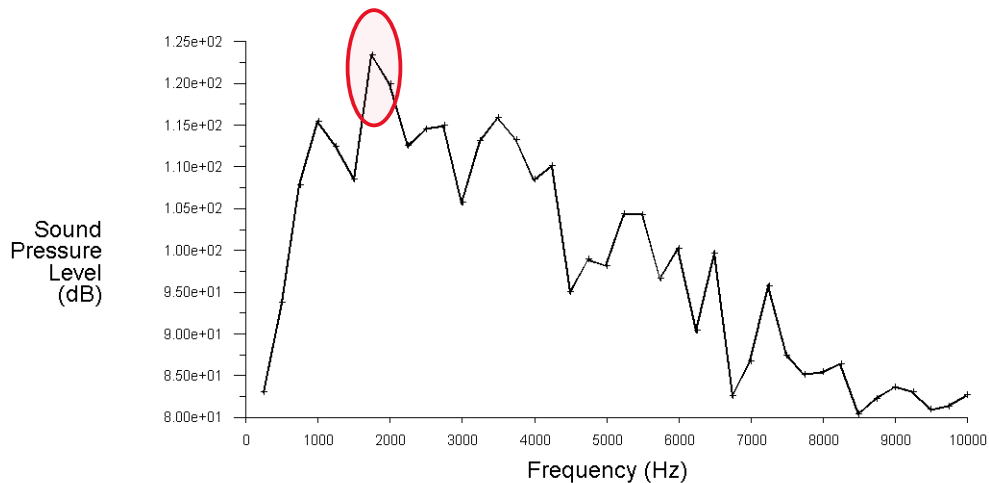


Fig.4.13 Spectral Analysis of Mic-2

Analyzing the FFT plots of Microphone 1 and Microphone 2 which are placed on the nozzle lip, we can see the screech tone peaks in both the plots for each Mach numbers. This spike predicts the presence of screech tone modes in this experimental case setup. From fig 4.8 and fig 4.9 we can see the highest sound pressure peak between 6000-7000 Hz. This result approves approximately with the experimental data from the experiment done by Ponton and Seiner [2].

When we analyze for M=1.5 in fig 4.10 and fig 4.11 we can see the peak between 4000-5000 Hz and around 2000 Hz for M=1.8 from fig 4.12 and 4.13. This shows that with increase in Mach numbers for an under expanded supersonic jet at a given inlet diameter, the screech tone peaks are obtained at lower frequencies.

## CHAPTER 5

### CONCLUSION AND FUTURE SCOPE OF WORK

#### *5.1 Conclusion*

The problem statement that is being worked upon is the prediction of jet screech noise generated from a supersonic jet nozzle exit at different Mach numbers. As mentioned earlier in the report, there lacks a mathematical formula for intensity calculation and determining the direction of screech tone. Research is being carried out extensively to predict the screech tone accurately and precisely when compared with the experimental data taken from Ponton and Seiner[2].

- A realizable k- $\epsilon$  viscous model has been applied in the simulation. This model is used because of its efficiency and accuracy.
- The steady-state analysis is used for optimizing the model, and the calibrated data is used for simulating the transient-state with changes in the settings for accuracy.
- Introducing a pressure-based solver in the simulation augments the results further.
- After the transient simulation, the microphone data is collected, and post-processing of the data is carried out.
- FFT plot with Sound pressure level on the y-axis and Frequency on the x-axis is taken into consideration for the Spectral analysis.
- It is observed from the FFT plot that between the frequency range of 6000Hz to 7000Hz for  $M = 1.2$ , there appears a spike in the sound pressure level which indicates the presence of screech tone in the free supersonic jet flow.
- Comparing between the frequency at which jet screech peaks are seen, we can summarize that with increase in Mach number, frequency at which the peak is obtained decreases
- Mach contours shows that with increase in  $M$ , the strength of shock waves decreases and the Mach cone width decreases making it narrower
- 

#### *5.2 Future scope of work*

This simulation is used as a test case which enables to work further in prediction of screech tone. Further future works can be to understand better about screech tone behaviours in the following ways.

- Introduction of sound reflecting plates or impingements by placing them in the upstream direction from the inlet and verify how the mach contours, screech tone behaviors changes with it. Comparison studies with different distances with respect to the jet inlet can be done, placing the impingement at various angle along the axis can be further improvements.

- It is important to have the correct turbulence model to obtain reliable CFD results. The simulations were done for the supersonic jets based on Reynolds Averaged Navier Stokes model in our project which was for near wall calculations. Considering other factors like Computational costs, Degree of freedom, Geometrical Complexity, Modelling Importance, advanced levels of models are present like Large Eddy Simulation model (LES), Detached Eddy Simulation model (DES), Hybrid RANS-LES models which offers higher applicability range and fidelity increase but computational costs are higher because these models are to be simulated at higher time steps.

## REFERENCE

- [1] A. T. Thies and C. K. W. Tam, "Computation of turbulent axisymmetric and nonaxisymmetric jet flows using the K- $\epsilon$  model," *AIAA Journal*, vol. 34, no. 2, pp. 309–316, 1996, doi: 10.2514/3.13065.
- [2] M. K. Ponton and J. M. Seiner, "THE EFFECTS OF NOZZLE EXIT LIP THICKNESS ON PLUME RESONANCE," 1992.
- [3] S. A. E. Miller and P. J. Morris, "The Prediction of Broadband Shock-Associated Noise from Dualstream and Rectangular Jets using RANS CFD."
- [4] P. J. Morris and S. A. E. Miller, "The Prediction of Broadband Shock-Associated Noise Using RANS CFD," 2009.
- [5] K. A. Kurbatskii, "Scale-Resolving Simulation of an Unsteady Turbulent Flow and Acoustic Field of a Screeching Supersonic Jet," 2012.
- [6] K. A. Kurbatskii, "Numerical Simulation of Three-Dimensional Jet Screech Tones using a General-Purpose Finite-Volume CFD code," 2011.
- [7] R. Gojon and C. Bogey, "Effects of the angle of impact on the aeroacoustic feedback mechanism in supersonic impinging planar jets," *International Journal of Aeroacoustics*, vol. 18, no. 2–3, pp. 258–278, Apr. 2019, doi: 10.1177/1475472X18812808.
- [8] H. Shen and C. K. W. Tam, "Numerical simulation of the generation of axisymmetric mode jet screech tones," *AIAA Journal*, vol. 36, no. 10, pp. 1801–1807, 1998, doi: 10.2514/2.295.
- [9] G. Sinibaldi, G. Lacagnina, L. Marino, and G. P. Romano, "Aeroacoustics and aerodynamics of impinging supersonic jets: Analysis of the screech tones," *Physics of Fluids*, vol. 25, no. 8, Aug. 2013, doi: 10.1063/1.4819333.
- [10] "Flow field and noise characteristics of a supersonic impinging jet," 1999.
- [11] P. R. Spalart, "Strategies for turbulence modelling and simulations." [Online]. Available: [www.elsevier.com/locate/jjh](http://www.elsevier.com/locate/jjh)
- [12] T. D. Norum, "Screech suppression in supersonic jets," *AIAA Journal*, vol. 21, no. 2, pp. 235–240, 1983, doi: 10.2514/3.8059.
- [13] C. K. W. Tam, H. Shen, and G. Raman, "Screech tones of supersonic jets from bevelled rectangular nozzles," *AIAA Journal*, vol. 35, no. 7, pp. 1119–1125, 1997, doi: 10.2514/2.232.
- [14] C. K. W. Tam, "SUPERSONIC JET NOISE," 1995. [Online]. Available: [www.annualreviews.org](http://www.annualreviews.org)
- [15] G. Sinibaldi, G. Lacagnina, L. Marino, and G. P. Romano, "Aeroacoustics and aerodynamics of impinging supersonic jets: Analysis of the screech tones," *Physics of Fluids*, vol. 25, no. 8, Aug. 2013, doi: 10.1063/1.4819333.

- [16] B. A. Powell and C. E. by J Richards, “On the Mechanism of Choked Jet Noise\*.”
- [17] H. Shen and C. K. W. Tam, “Numerical simulation of the generation of axisymmetric mode jet screech tones,” *AIAA Journal*, vol. 36, no. 10, pp. 1801–1807, 1998, doi: 10.2514/2.295.
- [18] NORUM, T. D. (1983). Screech suppression in supersonic jets. *AIAA Journal*, 21(2), 235–240. doi:10.2514/3.8059
- [19] Tam, C K W (1995). *Supersonic Jet Noise.* , 27(1), 17–43. doi:10.1146/annurev.fl.27.010195.000313
- [20] [www.afs.enea.it](http://www.afs.enea.it)
- [21] [www.idealsimulations.com](http://www.idealsimulations.com)
- [22] [www.wikipedia.org](http://www.wikipedia.org)